GEOPHYSICAL RESEARCH LETTERS, VOL. 33, L18707, doi:10.1029/2006GL027232, 2006

Click Here for Full Article

A Lagrangian identification of major sources of Sahel moisture

Raquel Nieto,[1,2] Luis Gimeno,[1,2] and Ricardo M. Trigo[2,3]

Received 14 June 2006; revised 20 July 2006; accepted 11 August 2006; published 27 September 2006.

[1] The drying trend in the Sahelian region from the 1950s to the 1990s was a hotspot of decadal-scale changes in the climate of the 20th century. However, the sources of moisture in this region have been poorly studied. Motivated by the excellent skills of a new Lagrangian method of diagnosis for identifying the sources of moisture over a region (Stohl and James, 2004, 2005), this study examines the main sources over the Sahel. The method computes budgets of evaporation minus precipitation by calculating changes in the specific humidity along the trajectories. We tracked the air masses residing over the Sahel over a period of five years (2000–2004). Recycling was identified as the major source of moisture over the Sahel. Two additional sources of moisture reaching Sahel have been identified here, namely; 1) a band in the North Atlantic stretching between the Sahel and Iberia, and 2) the entire Mediterranean basin, and the nearby Red Sea. **Citation:** Nieto, R., L. Gimeno, and R. M. Trigo (2006), A Lagrangian identification of major sources of Sahel moisture, *Geophys. Res. Lett.*, *33*, L18707, doi:10.1029/2006GL027232.

1. Introduction

[2] The Sahelian region is semi-arid, highly vulnerable to climate variability, and has experienced large decadal fluctuations in rainfall, including prolonged periods of drought. In the second half of the 20th century, the Sahel experienced two very different periods: the 1950s and 1960s were anomalously wet, while the 1970s and 1980s were anomalously dry [*Dai et al.*, 2004]. At least three possible explanations for this decline in rainfall have been suggested: (i) the effect of human activity on the surface vegetation [*Xue and Shukla*, 1993; *Clark et al.*, 2001], (ii) variations in sea surface temperatures (SSTs) over all the tropical oceans [*Lough*, 1986; *Giannini et al.*, 2003; *Folland et al.*, 1986; *Palmer*, 1986; *Thiaw and Bell*, 2005] and the Mediterranean [*Rowell*, 2003], and (iii) variations in the mean sea level pressure (MSLP) over the Sahara [*Haarsma et al.*, 2005], related to the global distribution of surface air temperature (SAT). The first hypothesis has traditionally been regarded as the primary cause for the drought, but recent modelling studies suggest that this trend was probably caused primarily by SST fluctuations. Decadal fluctuations in Sahel rainfall over the last 50 years are well reproduced in simulations with atmospheric GCMs forced by observed SSTs [*Giannini et al.*, 2003; *Bader and Latif*, 2003]. Models suggest that the land-surface feedbacks amplify the SST-induced changes [*Taylor et al.*, 2002; *Zeng et al.*, 1999].

[3] The abovementioned factors regarding the possible causes of interdecadal precipitation variability have been the focus of much climate research. However, the work reported here has a different focus. It is necessary to consider the precise *source* of the moisture when considering the causes of fluctuations in precipitation, as there is no precipitation without a supply of moisture. As noted by *Trenberth et al.* [2003. p. 1206] "this aspect of precipitation is one that has been underappreciated and is worthy of more attention." Although the Sahelian region is not an exception in this respect, we know the importance, as a source of the atmospheric moisture, of the soil moisture over (i) the Sahel (primary contribution to the recycling) [see, e.g., *Gong and Eltahir*, 1996; *Koster et al.*, 2004], (ii) the tropical North Atlantic [see, e.g., *Gong and Eltahir*, 1996; *Fontaine et al.*, 2003], (iii) the southern tropical Atlantic [e.g., *Thiaw et al.*, 1998] and (iv) the Mediterranean Sea [e.g., *Fontaine et al.*, 2003; *Rowell*, 2003]. A specific analysis that confirms/refutes the importance of these sources and identifies others, using well-developed Lagrangian methods of diagnosis, has not been performed for the Sahel region and is a major objective of this paper.

[4] In a two-paper work, *Stohl and James* [2004, 2005] applied a Lagrangian method of diagnosis to determine the source of moisture in a basin. It is based on meteorological analysis data, a particle dispersion model, and a Lagrangian analogue to the Eulerian budget method for diagnosing the surface moisture flux. Details of the method are provided in the work cited.

[5] Therefore, the main objective of this paper is to exploit this new Lagrangian method of diagnosis to identify the main sources of moisture and precipitation over the Sahel, by backward tracking the air masses that ultimately reach the Sahel.

2. Data and Methods

[6] Our study is based on the method developed by *Stohl and James* [2004, 2005], which uses the Lagrangian particle dispersion model FLEXPART [*Stohl et al.*, 1998] and meteorological analysis data from the European Centre for Medium-Range Weather Forecasts (ECMWF) (P. W. White (Ed.), IFS documentation, European Centre for Medium-Range Weather Forecasts, Reading, UK, 2002, available at http://www.ecmwf.int) to track atmospheric moisture along trajectories. The atmosphere is divided homogeneously into a large number of so-called particles and then these particles are transported by the model using three-dimensional winds, with their positions and specific humidity (q) being recorded every six hours. The increases (e) and decreases (p) in moisture along the trajectory can be calculated through changes in (q) with time ($e - p = m\ dq/dt$), (m) being the mass of the particle. When adding ($e - p$) for all the particles residing in the atmospheric column over an

[1]Departamento de Física Aplicada, Facultad de Ciencias de Ourense, Universidad de Vigo, Ourense, Spain.
[2]University of Lisbon, CGUL IDL, Lisbon, Portugal.
[3]Universidade Lusófona, Departamento de Engenharias, Lisbon, Portugal.

0094-8276/06/2006GL027232$05.00

area, we can obtain (*E−P*), where the surface freshwater flux (*E*) is the evaporation and (*P*) the precipitation rate per unit area. The method can also track (*E−P*) from a region backward in time along the trajectories, choosing particles appropriate for finding sources of moisture and precipitation. Limitations of the method concern mainly to the trajectory accuracy and the fact that a time derivative of the humidity is used (unrealistic fluctuations in humidity could be considered as moisture fluxes). However, the use of large time periods minimizes the effects of such unrealistic fluctuations. Full details of the method and its limitations can be found in work by *Stohl and James* [2004, 2005].

[7] In the work reported here we used the tracks of 1,398,801 particles over a five-year period (2000–2004) computed using ECMWF operational analysis available every six hours (00, 06, 12 and 18 UTC) with a 1° × 1° resolution and all 60 vertical levels of the analysis. We traced (*E−P*) backwards from the Sahelian region (*10°–20°N lat*, *20°E–18°W lon*), limiting the transport times to 10 days, which is the average time that water vapour resides in the atmosphere [*Numaguti*, 1999]. All the particles residing over the Sahelian region were identified every six hours and tracked backwards for 10 days. For the first trajectory time step, all the target particles resided over the Sahel region and (*E−P*) is the region-integrated net freshwater flux. For subsequent trajectory time steps, (*E−P*) represents the net freshwater flux into the air mass travelling to the Sahelian region. We calculated (*E−P*) on a 1° × 1° grid and averaged over seasonal, annual and five-year periods. (E−P) values for specific days are labeled $(E-P)_n$ here, so $(E-P)_2$ shows where the moisture over the Sahel as received or lost on the second day of the trajectory and the total (E−P) integrated over days 1 to n is labeled $(E-P)_n$, so $(E-P)^{10}$ is the sum of days 1 to 10. The analysis of (*E−P*) values tells us where and when the moisture over the Sahel was received or lost.

3. Results

[8] The Lagrangian diagnostics for E, P and E-P were validated by comparing results with those obtained with the Eulerian method of *Stohl and James* [2004] (see their Figure 2 for E-P comparison and Figure 4 for precipitation comparison). They found an excellent agreement on a global basis for the year 2000. We have compared E-P results at the Sahel scale between the Lagrangian and Eulerian (Figure 1) methods for a two year period (2000–2001). The Eulerian results were taken from the analysis by Trenberth and Stepaniak (http://www.cgd.ucar.edu/cas/catalog/newbudgets/index.html#Sec7) that use NCAR-NCEP data and the typical Eulerian approach [*Trenberth and Guillemot*, 1998]. The good agreement shows that results are robust independently of methods, reanalysis and scale choices. We have also done a comparison of P results for the same two years period (2000–2001) obtained with the Lagrangian method and from the GPCP V1DD dataset from NASA (1-degree daily combination precipitation estimates (http://ingrid.ldeo.columbia.edu/SOURCES/.NASA/.GPCP/.V1DD) [*Huffman et al.*, 2001]. We have displayed in Figure 1c the isoline of 1mm/day to show that the Lagrangian method is able to reproduce fairly accurately the meridional gradient of precipitation. It is important to notice that the Lagrangian approach is not able to separate E and P. Therefore P has been calculated based on the computation of E − P whenever $E-P < 0$. This approach often leads to underestimate values of P. It is important to stress that precipitation data derived from satellite is usually affected by considerable uncertainty, so the obtained agreement seems to be satisfactory.

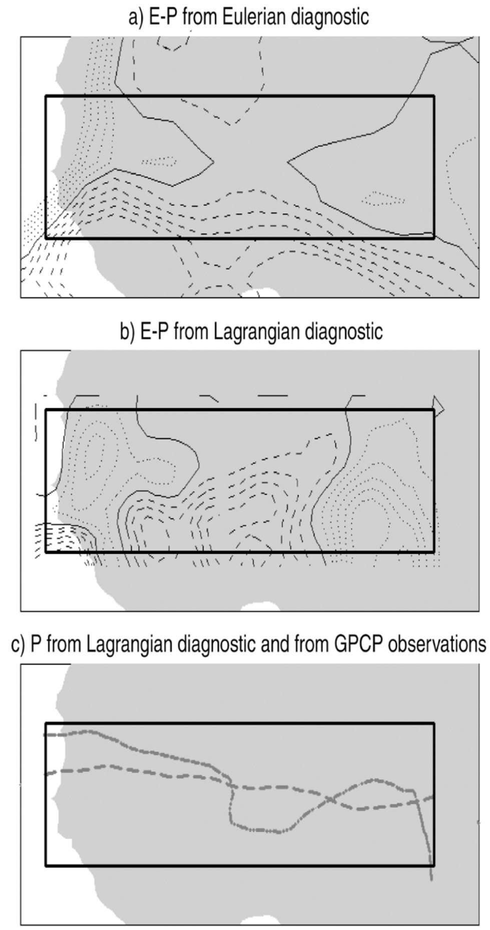

Figure 1. (a) The quantity E−P derived from the Eulerian diagnostic calculated from the NCEP/NCAR reanalysis (T42 spectral truncation on a 128 × 64 Gaussian grid). (b) The quantity E−P derived from the Lagrangian diagnostic based on ECMWF analyses. The interval of the data ranges from −1 and 1. Solid line corresponds to the 0 contour; dotted (dashed) line represents positive (negative) values; intervals for E−P = 0.2 mm/day. (c) 1 mm/day isoline of precipitation P derived from the Lagrangian diagnostic based on ECMWF analyses (solid line; calculated in a grid 1° × 1°) and GPCP observations (dashed line; calculated in a grid 1° × 1°). All figures were computed for the biennium 2000–2001.

[9] We tracked the air masses residing over the Sahel back in time to see where the moisture originated. Figure 2 shows the annually $(E-P)_n$ fields on the first, second, third, fifth, and tenth days of transport and averaged over all

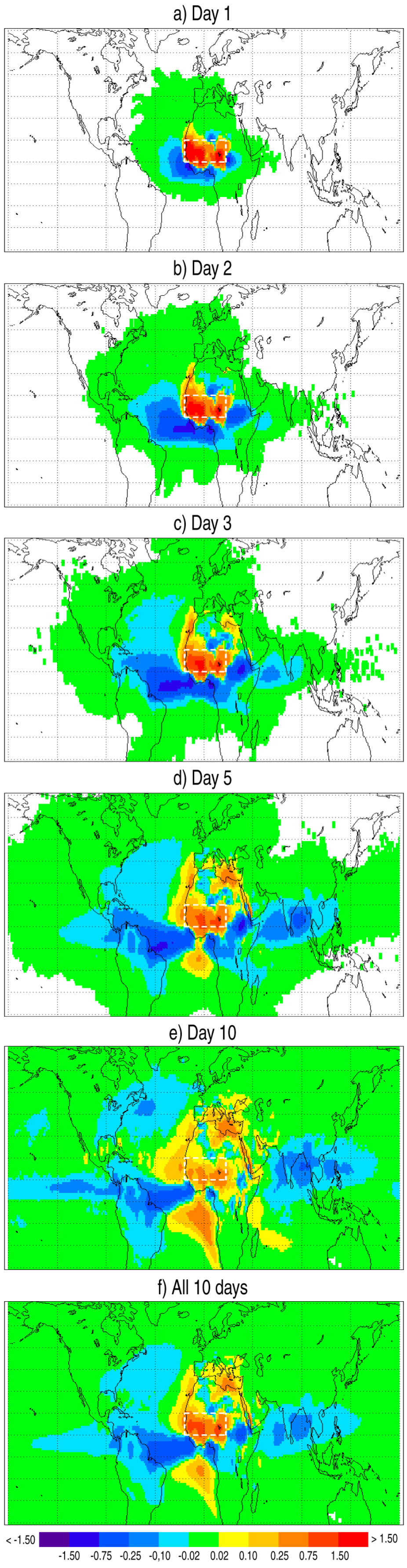

10 days $(E-P)^{10}$. One day back in time, all the air resided in the Northern Hemisphere and most of the air over the Sahel itself and surrounding areas. $(E-P)_1$ was negative over the Atlantic Ocean surrounding the Sahel, including the Guinea Gulf, which indicates that over this region convective precipitation typically occurs in air masses in transit to the Sahel (this area corresponds to the Intertropical Convergence Zone –ICZ-). The negative value over the continental area to the SE of the Sahel in Central Africa reveals an area of precipitation for air masses with origin in the Indian Ocean. $(E-P)_1$ was positive over the Sahel and the closest continental areas to the South in Central Sahel and to the North in Western Sahel, which indicates that the moisture over the Sahelian region receives a strong contribution from the soil moisture (in the Sahel, precipitation is affected significantly by soil moisture [see *Koster et al.*, 2004, Figure 1]. Similar source regions can be observed for $(E-P)_2$ with an expansion to the North over the North Africa Atlantic coast. This displacement continued in the third day of transport, with the Eastern Mediterranean appearing as a new source of moisture over the Sahel. It has been suggested in modelling studies that the Mediterranean source can explain fluctuations in the precipitation. *Rowell* [2003] commented that if SSTs in the Mediterranean are warmer than average, then local evaporation is enhanced and the moisture content of the lower troposphere increases, with the additional moisture being advected southward across the eastern Sahara by the mean flow reaching the Sahel. Similarly, the area with negative values of $(E-P)$ expanded in the third day of transport to the West and to the East along the ICZ. The pattern is slightly different for the fifth and tenth day of transport. The area with negative value of $(E-P)_5$ continued to expand along the Atlantic coast reaching the Iberian coasts and particles spread over most of the Mediterranean and the Red Sea. Particles crossing the ICZ continued to lose moisture, but there was a region in the tropical south Atlantic coast with positive value of $(E-P)_5$. This region expanded to the West and the South in the tenth day of transport. However, the negative values of $(E-P)_n$ for the first three days of transport in the ICZ area indicate that much of the moisture will be lost by precipitation during the three days before the air actually reaches the Sahel. Something similar will occur with the moisture produced in the area with positive value of $(E-P)_{10}$ over the Indian Ocean. Averaged over all 10 days of transport, there is a strong moisture uptake over the Sahel itself (which indicates the importance of recycling), the North Atlantic coasts up to Iberia, the Mediterranean area including the Red Sea, and the tropical South Atlantic Ocean, including the Guinea Gulf.

[10] Another interesting possibility with this Lagrangian method is to provide a quantification of the water vapour transport. More precisely it is appealing to evaluate the relative weight of the main source regions (i.e., Sahel-recycling-, the South Atlantic Ocean/the Guinea Gulf, the Eastern Mediterranean and the North Atlantic coast). We

Figure 2. Annually average $(E-P)_n$ fields of the Sahelian region from the backward tracking: (a) $(E-P)_1$, (b) $(E-P)_2$, (c) $(E-P)_3$, (d) $(E-P)_5$, (e) $(E-P)_{10}$, and (f) $(E-P)^{10}$ $(10\ \text{days})^{-1}$, i.e., averaged over 10 days back.

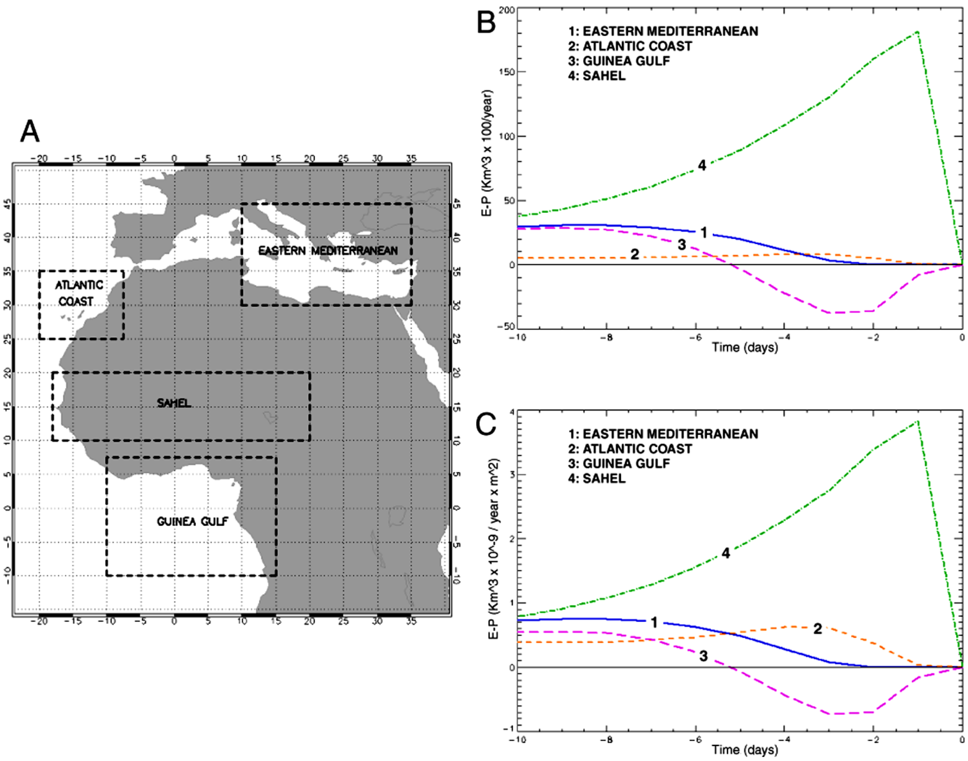

Figure 3. (a) Time series of $(E-P)_n$ calculated backward for moisture over the Sahel area and integrated over the regions indicated: Eastern Mediterranean Sea (curve 1), Atlantic Coast (curve 2), the South Atlantic Ocean/Guinea Gulf (curve 3) and the Sahel (curve 4). (b) Absolute values of $(E-P)_n$ time series (scale regulated by a factor of 100). (c) Relative values of $(E-P)_n$ time series, taking into account to the area of each region (scale regulated by a factor of 10^9).

have quantified $(E-P)_n$ series calculated backwards from the Sahel and integrated over these four regions (Figure 3). Figure 3a shows the limits of the source regions, Figure 3b depicts the values of $(E-P)_n$ without considering the different areas of each source region, and Figure 3c the corresponding values of $(E-P)_n$ divided by the appropriate area of the source regions. A view of Figure 3b shows that the Sahel itself is clearly the most important source up to 10 days back. It takes about 3 (6) days back for the Eastern Mediterranean (South Atlantic Ocean/Guinea Gulf) to become a relevant moisture source for the Sahel, being their importance very similar since 7 to 10 days back. The supply of moisture from the North Atlantic coasts, although always positive is less than the supply from the other main sources, due to its smaller size. Its relative importance is put in evidence analyzing $(E-P)_n$ values divided by the area of the source region (Figure 3c). In this case the Atlantic coast is the second more important source from 1 to 5 days back. In fact, using the normalised time series the four different sources present a smaller range of relative contribution for $(E-P)_{10}$, with the Eastern Mediterranean closing the gap to the Guinea Gulf.

[11] These patterns of the $(E-P)$ fields were very robust, so similar structures appeared when the analysis was done on a seasonal basis. Figure 4 shows the seasonal $(E-P)$ averaged over all 10 days of transport (winter, January–March; spring, April–June; summer, July–September, and autumn, October–December). There are differences concerning the area of moisture loss in the ICZ: it is mostly confined to the Atlantic and Africa during fall, slightly expanded to the Pacific during winter, expanded to the Indic Ocean and Indonesia during spring, and absent in the Atlantic, but included partly in the Sahelian area, during summer, when it is stronger in Asia. This behaviour is in clear agreement with the seasonal cycle of the West African monsoon. North of 8°N latitude, the seasonal cycle of precipitation consists of a single rainy season, which could be as brief as three months, from July to September in the Northern Sahel [*Lebel et al.*, 2003]. Other important differences occur during summer, the season when discrepancies are higher and when precipitations over the Sahel are more abundant. Figure 5 shows the summer $(E-P)_n$ fields on the first, second, third, fifth and tenth days of transport. Two points are worthy of note. First, $(E-P)_n$ is not completely positive over the target region, the Sahel, in the first three days of transport. This indicates that there are regions inside the Sahel where moisture actually increases, (mostly the western half) and other regions, mostly in the central part, where it decreases (areas with convective precipitation as $(E-P)_1$ is negative). This is concordant with the maximum occurrence of mesoscale convective complexes at 10°E [see *Lebel et al.*, 2003, Figure 7]. Second, unlike in winter, there is no area with a negative (E-P) value between the Sahel and the moisture source region in the South Atlantic. This means that the strong positive values of $(E-P)_3$, $(E-P)_5$ and $(E-P)_{10}$ over the South Atlantic indicate important sources of the Sahelian moisture. The positive values of $(E-P)_{10}$ over the southern Indian Ocean, although higher

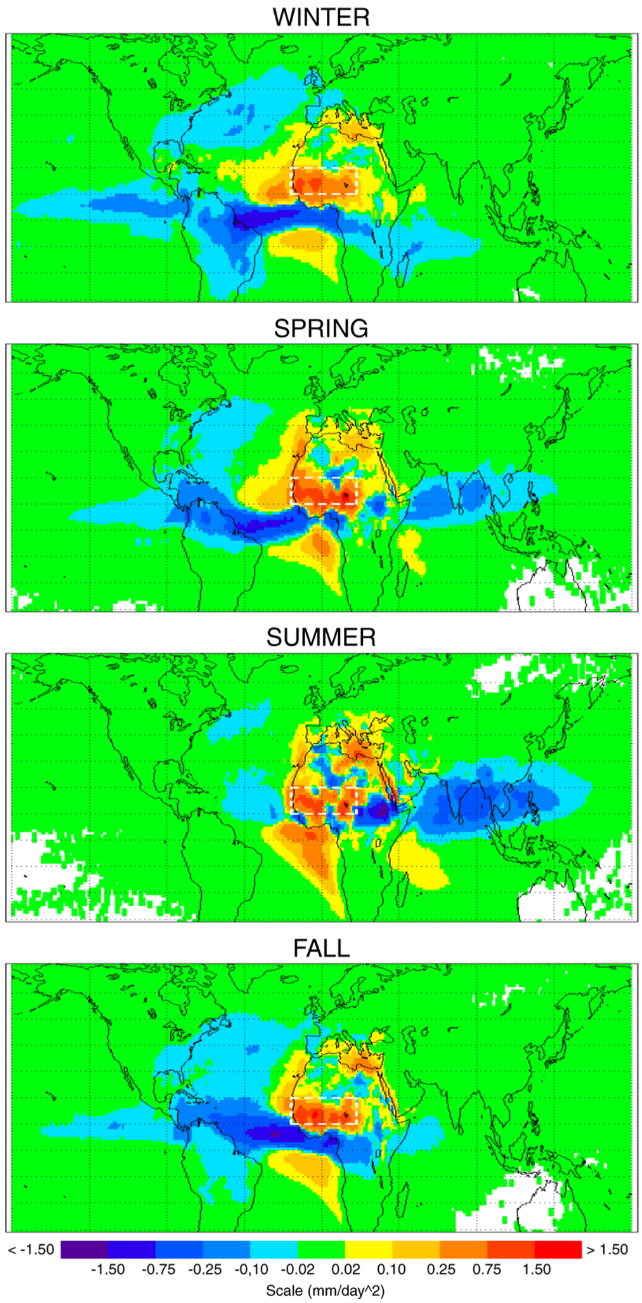

Figure 4. Seasonal average $(E-P)^{10}$ $(10 \text{ days})^{-1}$ fields of the Sahelian region from the backward tracking (winter, January–March; spring, April–June; summer, July–September, and autumn, October–December).

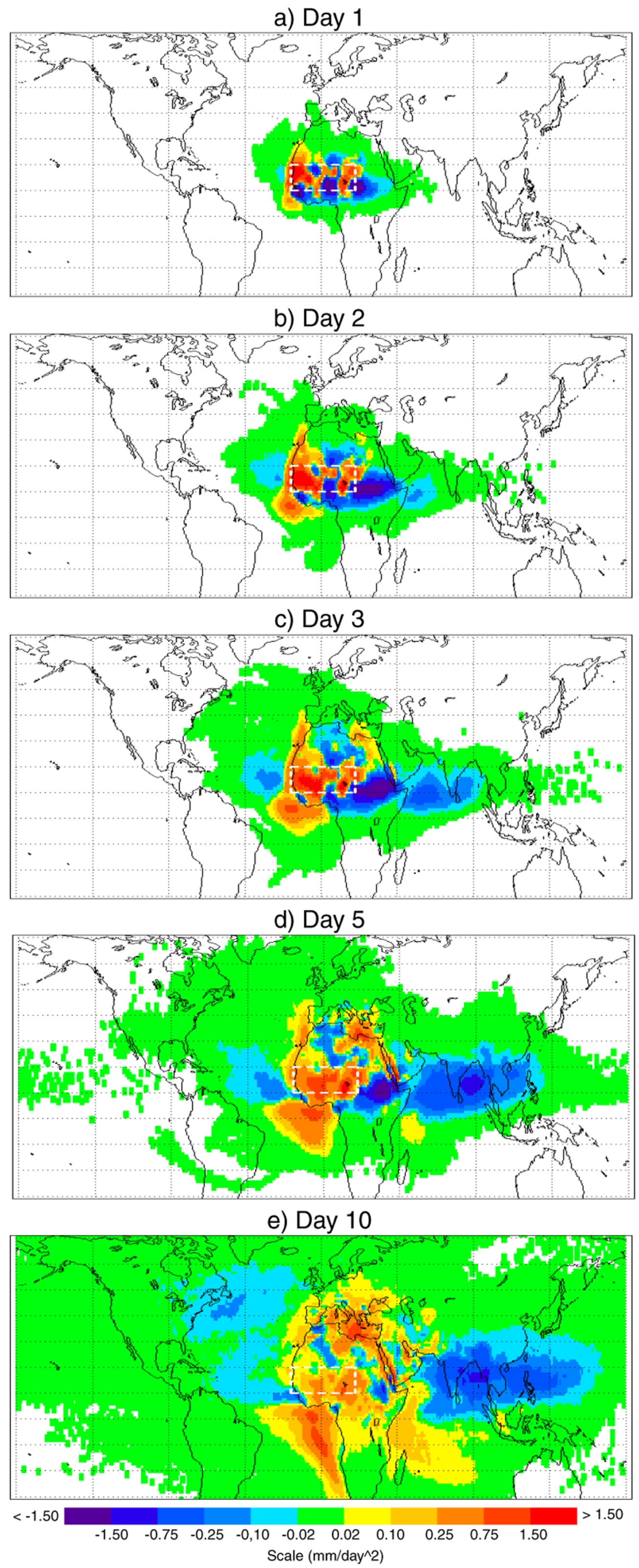

Figure 5. Summer average $(E-P)_n$ fields of the Sahelian region from the backward tracking: (a) $(E-P)_1$, (b) $(E-P)_2$, (c) $(E-P)_3$, (d) $(E-P)_5$, and (e) $(E-P)_{10}$.

than for the annual pattern, could not be associated with important moisture sources because of the negative values of $(E-P)$ in the first five days of transport.

4. Concluding Remarks

[12] An analysis of the major sources of moisture over the Sahel was performed, using a Lagrangian method of diagnosis. We studied the mean conditions over a five-year period (2000–2004), which can be considered typical on a global climate scale, because there were no extremes of climate variability, such as those associated to the El Niño-

Southern Oscillation (ENSO) or the North Atlantic Oscillation (NAO). As expected from previous related studies, recycling was found to be the dominant moisture source over the Sahel. This source is important during the first days of transport, and also on average over all 10 days of transport. A band along the North Atlantic from the Sahel latitudes to the Iberian coasts and the Mediterranean area, including the Red Sea, are the other two important sources of the Sahel moisture over the year as a whole. There is strong moisture uptake over the tropical South Atlantic following the fifth day of transport, as well as on average over the 10 days of transport. However, it is not a major source during autumn, winter and spring because of the loss of moisture by precipitation during the three days before the air reaches the Sahelian region. This last fact does not occur during summer, which is why the South Atlantic Ocean is an important source of summertime moisture over the Sahel. The Indian Ocean does not seem to be an important source, although it could have a minor influence during summer.

[13] **Acknowledgments.** We thank Andreas Stohl for providing the trajectory data and the Xunta de Galicia, the FCT of Portuguese Ministry of Science (SFRH/BPD/22178/2005) and the Spanish Ministry of Education and Science for granting the stays of R. Nieto and L. Gimeno in the "Centro de Geofísica da Univ. de Lisboa (CGUL-IDL)" through the programmes "Bolsas para estadias no estranxeiro" and "Programa Nacional de ayudas para la movilidad de profesores de universidad e investigadores españoles y extranjeros."

References

Bader, J., and M. Latif (2003), The impact of decadal-scale Indian Ocean sea surface temperature anomalies on Sahelian rainfall and the North Atlantic Oscillation, *Geophys. Res. Lett.*, *30*(22), 2169, doi:10.1029/2003GL018426.

Clark, D. B., Y. K. Xue, R. J. Harding, and P. J. Valdes (2001), Modeling the impact of land surface degradation on the climate of tropical North Africa, *J. Clim.*, *14*, 1809–1822.

Dai, A., P. J. Lamb, K. E. Trenberth, M. Hulme, P. D. Jones, and P. Xie (2004), The recent Sahel drought is real, *Int. J. Climatol.*, *24*, 1323–1331.

Folland, C. K., and T. N. Palmer (1986), Sahel rainfall and worldwide sea temperatures, *Nature*, *320*, 602–607.

Fontaine, B., P. Roucou, and S. Trzaska (2003), Atmospheric water cycle and moisture fluxes in the West African monsoon: Mean annual cycles and relationship using NCEP/NCAR reanalysis, *Geophys. Res. Lett.*, *30*(3), 1117, doi:10.1029/2002GL015834.

Giannini, A., R. Saravanan, and P. Chang (2003), Oceanic forcing of Sahel rainfall on interannual to inter-decadal time scales, *Science*, *302*, 1027–1030.

Gong, C., and E. A. B. Eltahir (1996), Sources of moisture for rainfall in West Africa, *Water Resour. Res.*, *32*(10), 3115–3121.

Haarsma, R. J., F. M. Selten, S. L. Weber, and M. Kliphuis (2005), Sahel rainfall variability and response to greenhouse warming, *Geophys. Res. Lett.*, *32*, L17702, doi:10.1029/2005GL023232.

Huffman, G. J., R. F. Adler, M. M. Morrissey, S. Curtis, R. Joyce, B. McGavock, and J. Susskind (2001), Global precipitation at one-degree daily resolution from multi-satellite observations, *J. Hydrometeorol.*, *2*, 36–50.

Koster, R. D., et al. (2004), Regions of strong coupling between soil moisture and precipitation, *Science*, *305*, 1138–1140.

Lebel, T., A. Diedhiou, and H. Laurent (2003), Seasonal cycle and interannual variability of the Sahelian rainfall at hydrological scales, *J. Geophys. Res.*, *108*(D8), 8389, doi:10.1029/2001JD001580.

Lough, J. M. (1986), Tropical Atlantic sea surface temperatures and rainfall variations in sub-Saharan Africa, *Mon. Weather Rev.*, *14*, 561–570.

Numaguti, A. (1999), Origin and recycling processes of precipitating water over the Eurasian continent: Experiments using an atmospheric general circulation model, *J. Geophys. Res.*, *104*, 1957–1972.

Palmer, T. N. (1986), Influence of the Atlantic, Pacific and Indian oceans on Sahel rainfall, *Nature*, *322*, 251–253.

Rowell, D. P. (2003), The impact of Mediterranean SSTs on the Sahelian rainfall season, *J. Clim.*, *16*, 849–862.

Stohl, A., and P. James (2004), A Lagrangian analysis of the atmospheric branch of the global water cycle. part 1: Method description, validation, and demonstration for the August 2002 flooding in central Europe, *J. Hydrometeorol.*, *5*, 656–678.

Stohl, A., and P. James (2005), A Lagrangian analysis of the atmospheric branch of the global water cycle. part 2: Earth's river catchments, ocean basins, and moisture transports between them, *J. Hydrometeorol.*, *6*, 961–984.

Stohl, A., M. Hittenberger, and G. Wotawa (1998), Validation of the Lagrangian particle dispersion model FLEXPART against large scale tracer experiment data, *Atmos. Environ.*, *32*, 4245–4264.

Taylor, C. M., E. F. Lambin, N. Stephenne, R. J. Harding, and R. L. H. Essery (2002), The influence of land use change on climate in the Sahel, *J. Clim.*, *15*, 3615–3629.

Thiaw, W. M., and G. D. Bell (2005), Mechanisms associated with the June–September 2003 Sahel rainfall and implications for seasonal climate forecasts, *CLIVAR Exchanges*, *10*(1), 293.

Thiaw, W. M., J. V. Kousky, and V. Kumar (1998), Atmospheric circulation associated with recent Sahelian hydrologic anomalies, *IAHS Publ.*, *252*, 63–67.

Trenberth, K. E., and C. J. Guillemot (1998), Evaluation of the atmospheric moisture and hydrological cycle in the NCEP/NCAR reanalysis, *Clim. Dyn.*, *14*, 213–231.

Trenberth, K. E., A. Dai, R. M. Rasmussen, and D. B. Parsons (2003), The changing character of precipitation, *Bull. Am. Meteorol. Soc.*, *84*, 1205–1217.

Xue, Y., and J. Shukla (1993), The influence of land surface properties on Sahel climate, part I: Desertification, *J. Clim.*, *6*, 2232–2244.

Zeng, N., J. D. Neelin, K. M. Lau, and C. J. Tucker (1999), Enhancement of interdecadal climate variability in the Sahel by vegetation interaction, *Science*, *286*, 1537–1540.

L. Gimeno and R. Nieto, Departamento de Física Aplicada, Facultad de Ciencias de Ourense, Universidad de Vigo, Ourense E-32004, Spain. (l.gimeno@uvigo.es)

R. M. Trigo, Centro de Geofísica da Universidade de Lisboa, Departamento de Fisica, Faculdade de Ciencias, Universidade de Lisboa, P-1749-016, Lisboa, Portugal.